J. Med. Plants 2025; 24(96): 22-36

Institute of Medicinal Plants

Journal of Medicinal Plants

Journal homepage: www.jmp.ir

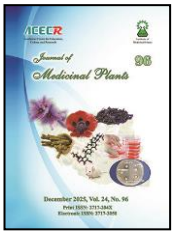

Research Article

Green synthesis of gold nanoparticles using *Zataria multiflora* Boiss. extract and evaluation of antibacterial activity

Fariba Mahmoudi[1], Parichehr Hanachi[1,*], Reza Falak[2,3], Ali Mohammadi[4]

[1] *Department of Biotechnology, Faculty of Biological Sciences, Alzahra University, Tehran, Iran*

[2] *Immunology Research Center, Iran University of Medical Sciences, Tehran, Iran*

[3] *Department of Immunology, School of Medicine, Iran University of Medical Sciences, Tehran, Iran*

[4] *Department of Microbiology, Faculty of Biological Sciences, Alzahra University, Tehran, Iran*

ARTICLE INFO

Keywords:
Biological synthesis
Gold nanoparticles
Antimicrobial activity
Zataria multiflora
Flavonoids
Phenols
Plant extracts

ABSTRACT

Background: Nanoparticle applications are expanding across biomedical research. Plant extract–mediated (green) synthesis offers a sustainable and economically viable route for nanoparticle production. **Objective:** This study focused on the synthesis of gold nanoparticles (AuNPs) using *Zataria multiflora* Boiss extract and evaluated their antibacterial efficacy. **Methods:** AuNPs were synthesized using the aqueous extract of the *Z. multiflora* plant. The nanoparticles were characterized by UV–Vis spectroscopy, energy-dispersive X-ray analysis (EDAX), transmission electron microscopy (TEM), scanning electron microscopy (SEM), Fourier-transform infrared spectroscopy (FTIR), dynamic light scattering (DLS), and zeta-potential measurements. The total phenolic content of the *Z. multiflora* extract was quantified using a gallic acid standard curve. Flavonoid content was measured using quercetin as the standard. Antioxidant capacity was assessed with ascorbic acid as the reference standard. The antibacterial activity of the synthesized AuNPs was evaluated by determining the minimum inhibitory concentration (MIC), minimum bactericidal concentration (MBC), and by disk diffusion assays. **Results:** Spectroscopy showed a peak for AuNPs at 530 nm. DLS revealed an average hydrodynamic diameter of 123.8 nm with a moderate size distribution. The zeta-potential was highly negative (-77.7 mV), indicating colloidal stability. AuNPs exhibited significant antibacterial activity against both *S. aureus* and *E. coli* in MIC, MBC, and disk diffusion assays. **Conclusion:** *Z. multiflora* extract effectively mediates the biosynthesis of stable AuNPs with notable antibacterial activity, supporting its potential for green nanomaterial synthesis in antimicrobial applications.

Abbreviations: AuNPs, Gold nanoparticles; DLS, Dynamic light scattering; DPPH, 2,2-Diphenyl-1-picrylhydrazyl; EDAX, Energy dispersive X-ray analysis; FTIR, Fourier-transform infrared spectroscopy; GAE, Gallic acid equivalent; MBC, Minimum bactericidal concentration; MIC, Minimum inhibitory concentration; OD, Optical density; SEM, Scanning electron microscopy; TEM, Transmission electron microscopy; TFC, Total flavonoid content; TPC, Total phenolic content.

*Corresponding author: p.hanachi@alzahra.ac.ir

doi:

Received 16 August 2025; Received in revised form 19 October 2025; Accepted 5 November 2025

1. Introduction

Nanoparticles (NPs) have garnered significant attention in biomedical research due to their versatile properties, which enable applications in drug delivery, diagnostics, and therapeutic interventions. Among them, gold nanoparticles (AuNPs) stand out because of their unique optical characteristics, excellent biocompatibility, low toxicity, and chemical stability. Additionally, AuNPs resist surface oxidation and can be readily functionalized, further enhancing their potential for diverse biomedical applications. [1]. The biological activity of NPs is largely determined by their size and structure. This activity is further affected by environmental conditions and the procedure of synthesis [2]. NPs have small size, similar to biomolecules such as proteins and DNA, which makes them suitable carriers for application in bioassays and drug delivery, unlike larger carriers such as liposomes, which exhibit limited cellular uptake [3]. Different physical and chemical methods can be used to create nanoparticles [4]. However, these methods are often environmentally unfriendly, as they require toxic solvents and harmful compounds. They are also expensive and can generate additional hazardous byproducts. Consequently, biosynthetic approaches for nanoparticle production have gained considerable interest in recent years. Green synthesis is environmentally friendly, simple, single-step, efficient, and cost-effective [5, 6]. This strategy employs biological agents, including microorganisms, plants, and enzymes, for nanoparticle synthesis. Among these agents, plants have been more popular due to their cost-effectiveness and the lack of need for complex maintenance of cell cultures, which makes them suitable for large-scale production [5]. Plant secondary metabolites influence nanoparticle synthesis, acting as natural reducing and stabilizing agents. Compounds like proteins, polysaccharides, flavonoids, terpenoids, and phenolic acids make this method environmentally safer by reducing the need for toxic chemicals [2, 7]. *Zataria multiflora* Boiss is a popular Iranian medicinal plant and a member of the Lamiaceae family. Studies have reported that this plant possesses numerous biomedical properties, including anticancer, anti-inflammatory, antioxidant, and antimicrobial characteristics [8]. The key bioactive compounds in *Z. multiflora* are phenolic phytochemicals such as carvacrol, thymol, and eugenol. In addition, p-cymene is reported as the principal non-phenolic constituent of this plant [9]. According to studies, various phytochemicals in *Z. multiflora* can affect the morphology and dimensions of the synthesized nanoparticles. AuNPs synthesized using *Z. multiflora* extract have been reported to produce nanoparticles with sizes within a range suitable for biomedical applications. Biomolecules of the plant extract play a key role in nanoparticle synthesis by enabling their formation and ensuring their stability. Proteins enhance stability, while phenolic compounds bind metals through hydroxyl and carboxyl groups [10, 11].

Many studies have demonstrated that, AuNPs play important roles in biology and environmental applications as antibacterial and antifungal agents [12, 13]. Given that *Z. multiflora* has potent antibacterial and antioxidant properties, it was chosen to prepare antibacterial gold nanoparticles in the present project. In this study, AuNPs were synthesized by the green synthesis method using *Z. multiflora* aqueous extract and subsequently characterized. Antibacterial effects of synthesized AuNPs were evaluated by minimum

inhibitory concentration (MIC), minimum bactericidal concentration (MBC), and disk diffusion assays.

2. Materials and methods

This study was approved by the Ethics Committee of Alzahra University, Tehran, Iran (Approval ID: IR.ALZAHRA.REC.1402.015; Date: 2023-05-17).

2.1. Preparation of Zataria multiflora aqueous extract

The aerial parts of *Zataria multiflora* Boiss were purchased from the Medicinal Plants Garden of Firouzeh, Tehran, Iran. The plant identity was confirmed by comparison with authenticated herbarium specimens at the Herbarium of the Faculty of Biological Sciences, Alzahra University, Tehran, Iran (Herbarium code: ALUH). Five grams of dried plant leaves were mixed with 100 ml of sterile distilled water, boiled for 3 min, and stirred for 10 min at 60 °C. After filtration with Whatman No. 1 filter paper, the extract was stored at 4 °C until further application [14].

2.2. Total phenolic content

The Folin–Ciocalteu colorimetric method was employed to determine the total phenolic content (TPC), as outlined previously by Meamari et al. (2022) with minor modifications. Gallic acid was employed to generate the standard calibration curve (Merck, Germany) (10, 20, 30, 40, and 50 µg/ml). For each measurement, 200 µl of *Z. multiflora* extract or standard was mixed with 200 µl of 10 % Folin–Ciocalteu reagent (Merck, Germany) (diluted with distilled water) and kept at room temperature (RT). After 5 min, 100 µl of 7 % sodium carbonate (Na_2CO_3, DYC, Iran) solution and 1.8 ml of distilled water were added. The tubes were incubated in a dark place at RT for 90 min. Absorbance was measured at 765 nm using an ultraviolet (UV)-visible spectrophotometer (Potonix Ar 2017, UK). The phenolic content was calculated by plotting a calibration curve and applying the resulting linear equation ($y = 0.1919x - 0.2082$; $R^2 = 0.9822$). Results were reported in milligrams of gallic acid equivalent per gram of dry weight (mg GAE/g DW) (mean ± SD). All experiments were conducted in triplicate [15].

2.3. Total flavonoid content

Total flavonoid content (TFC) was determined through a colorimetric assay based on aluminum chloride ($AlCl_3 \cdot 6H_2O$). A standard calibration curve was prepared using quercetin (Sigma, USA) (10, 20, 30, 40, and 50 µg/ml). For each measurement, 200 µl of *Z. multiflora* extract or standard was mixed with 100 µl of 10 % aluminum chloride ($AlCl3 \cdot 6H_2O$, Merck, Germany) and 100 µl of 1 M potassium acetate (Chemex, Iran) solutions. DW was added to get a final volume of 3 ml. The tubes were incubated in the dark for 30 min at RT. Using a UV–visible spectrophotometer, absorbance at 415 nm was measured, and a calibration curve was constructed to calculate flavonoid content via the linear equation ($y = 0.0993x - 0.0946$; $R^2 = 0.9955$). Results were expressed as mg quercetin equivalent per gram of dry weight (QE/g DW) of the extract (mean ± SD). All measurements were performed in triplicate [16].

2.4. Antioxidant capacity

The antioxidant capacity of *Z. multiflora* extract was assessed with two methods, including DPPH (2,2-diphenyl-1-picrylhydrazyl) radical scavenging assay based on a standard curve of ascorbic acid (Sigma, USA), and percentage inhibition of DPPH radicals.

For the ascorbic acid standard curve, a stock solution of 1 mM concentration was made using distilled water, and working standards were made accordingly (5-30 µg/ml). Fresh 0.1 mM DPPH (Sigma, USA) solution in methanol (Merck, Germany) was used. Each standard (1 ml) was mixed with 2 ml DPPH, vortexed, and incubated in the dark at room temperature for 30 minutes, and absorbance was recorded at 517 nm. A blank with DPPH in methanol served as a negative control. A calibration curve was plotted ($y = 0.1023x - 0.147$, $R^2 = 0.9818$), and the antioxidant capacity was reported as µmol ascorbic acid equivalent per gram of dried weight (AAE/g DW) [17].

The percentage of DPPH radical scavenging was used to further assess the antioxidant capacity [18]. One millilitre of the extract was added to 2 ml of DPPH, vortexed, and incubated in the dark for 30 min at RT. Ascorbic acid and DPPH without extract served as positive and negative controls, respectively. Absorbance was measured at 517 nm. The percentage of inhibition was determined as % DPPH radical inhibition = $[(Abs_{Control} - Abs_{sample})/Abs_{Control}] \times 100$, where $Abs_{Control}$ was the absorbance of DPPH without extract, and Abs_{Sample} was the absorbance with extract. Measurements were done in triplicate, and results were expressed as mean ± SD.

2.5. Biosynthesis and characterization of AuNPs

To synthesize Zataria-AuNPs, 10 ml of 1 mM $HAuCl_4$ (Sigma, USA) was added to different volumes of *Z. multiflora* leaf extract (0.1, 0.5, and 1.0 ml), resulting in final $HAuCl_4$ concentrations of approximately 0.990, 0.952, and 0.909 mM, respectively. The reaction mixture was stirred at 300 rpm at 80 °C for 20 min at pH 7. The color change to ruby red confirmed the formation of AuNPs, with the extract acting as a reducing agent, converting Au^{3+} to Au^0 [14]. Positive controls ($HAuCl_4$ without extract) and negative controls (extract without $HAuCl_4$) were included to confirm the role of the extract in nanoparticle formation. The Zataria-AuNPs suspension was centrifuged for 30 minutes at 9,000 rpm (Hettich, Germany). The Zataria-AuNPs was washed three times with distilled water after the supernatant was disposed of. Next, a small quantity of deionised water was used to dissolve Zataria-AuNPs. The concentrated Zataria-AuNP combination was vortexed for three minutes and sonicated for thirty minutes to create a homogenised mixture [16].

The synthesis of AuNPs was verified using UV-visible spectroscopy after mixing $HAuCl_4$ with three volumes of extract (0.1, 0.5, and 1.0 ml). Dynamic light scattering (DLS, Malvern Instruments, UK) was used to assess the particle size distribution and Zeta-potential at 25 °C. Energy-dispersive X-ray spectroscopy (EDAX) (EDS SAMX, France) determined elemental composition and the presence of capping elements. The morphology, shape, and size of the AuNPs were examined by transmission electron microscopy (TEM, LEO 906E, Germany) and scanning electron microscopy (SEM, MIRA3 TESCAN, Czech Republic). All measurements were performed in triplicate to ensure the accuracy and reproducibility of the results. To identify the functional groups on the nanoparticle surface, Fourier-transform infrared (FTIR, Bruker, Germany) spectroscopy was conducted using the KBr pellet method (sample: KBr ratio of 1:100), with spectra recorded in the range of 500 – 4000 cm^{-1}.

2.6. Antibacterial activity of Zataria-AuNPs

In order to investigate the antimicrobial activity of Zataria-AuNPs against common gram-positive (*Staphylococcus aureus,* ATCC

29213) and gram-negative (*Escherichia coli*, ATCC 25922) bacteria, Kirby-Bauer disk diffusion assay, MIC, and MBC methods were employed.

2.7. Disc diffusion assay

Bacterial inoculum was grown in Mueller-Hinton broth (Quelab, Canada). The suspension was standardized to 0.5 McFarland and inoculated onto Mueller-Hinton agar (Quelab, Canada) plates. Different concentrations of Zataria-AuNPs (50, 100, 200, and 300 µg/ml) were prepared by dissolving the lyophilized NPs in sterile Milli-Q water (DAcell, Iran). Sterile discs containing Zataria-AuNPs (50–300 µg/ml) were placed on the inoculated plates. Tobramycin discs (for *E. coli*) and tazobactam discs (for *S. aureus*) (Padtan Teb, Iran) were used as positive controls, while blank discs served as negative controls. The plates were incubated at 37 °C, and inhibition zones were measured after 20 h. Medium quality was visually inspected before use.

2.8. MIC and MBC

To determine the MIC of Zataria-AuNPs, the micro-broth dilution assay was conducted following CLSI guideline #M07-A8, and a serial dilution of NPs was prepared at final concentrations of 600, 300, 150, 75, 37.5, 18.7, 9.3, 6.6, 2.3, and 1.1 µg/ml, In a 96-well plate. A bacterial suspension adjusted to the 0.5 McFarland standard was dispensed into each well, and serial dilutions of the NPs were added accordingly. After 18 h of incubation at 37 °C, the lowest concentration of NPs that showed no visible turbidity was recorded as the MIC. A microplate reader (BIOHIT BP800, Finland) was used to measure the optical density (OD) at 600 nm in order to confirm the visual assessment of bacterial growth suppression. To determine the MBC, 10 µl of the content of the wells that showed no visible growth in the MIC assay was subcultured onto Mueller-Hinton agar plates and incubated at 37 °C for 18 h. The lowest concentration of Zataria-AuNPs that resulted in no colony formation on the agar surface was considered the MBC.

2.9. Statistical analysis

All experiments were performed in triplicate, and results are presented as mean ± SD. Statistical significance was evaluated using t-test and one-way ANOVA, with $P < 0.05$ considered significant. Analyses were carried out using GraphPad Prism 9.0 (GraphPad Software, USA).

3. Results

3.1. Total phenolic and flavonoid content of the Z. multiflora aqueous extract, and its antioxidant activity

The mean ± SD of the total phenolic content of *Z. multiflora* aqueous extract based on gallic acid equivalents per gram of dried extract was 5.46 ± 0.40 mg GAE/g DW. Similarly, its total flavonoid content based on quercetin equivalents per gram of the dried extract was 61.27 ± 1.40 mg QE/g DW.

Based on ascorbic acid equivalence measurement, the total antioxidant capacity was 16.01 ± 1.06 µmol AAE/g DW, and based on measurement of the inhibition of DPPH radicals, it was 17.33 ± 1.15 %, indicating its moderate antioxidant potential.

3.2. Synthesis and characterization of the Zataria-AuNPs

Three different volumes of the extract were used to synthesize AuNPs. Given that the purple color shift is one of the key indicators verifying the synthesis of AuNPs, through the process

[19], the most visible purple color was observed with the addition 0.1 ml of the extract, while higher extract volumes produced darker shades. This color change suggests that 0.1 ml of this extract is an ideal concentration for synthesis of the desired NPs.

3.3. UV-Visible spectroscopy

UV–visible spectroscopy verified the synthesis of AuNPs. The spectra indicated that extract volume significantly influenced gold ion reduction (Fig. 1a-c). With 0.1 ml extract, a typical SPR peak appeared at 530 nm, consistent with the purple color of AuNPs. In contrast, higher volumes (0.5 and 1 ml) produced absorption peaks at 450 and 430 nm, respectively—outside the typical SPR range (515 – 550 nm)—and a dark green color, suggesting incomplete nanoparticle formation under those conditions.

3.4. Morphological characteristics

The TEM and SEM micrographs exhibited that the synthesized AuNPs have spherical shape. The NPs size based on TEM studies ranged between 10 to 20 nm. The average particle size was 14.70 ± 3.46 nm, while SEM images showed a size range of 30 to 100 nm. The average particle size was 46.58 ± 25.36 nm (Fig. 2a-f), possibly due to particle aggregation during sample preparation.

3.5. DLS and Zeta-potential studies

The average hydrodynamic diameter of Zataria-AuNPs were 123.8 ± 32.1 nm (Fig. 3a) with a Polydispersity Index (PDI) value of 0.262, indicating a moderate size distribution. Zeta-potential of the Zataria-AuNPs were -77.7 mV (Fig. 3b). This high negative surface charge potential indicates that the synthesized AuNPs are electrostatically stabilized, suggesting a uniform dispersion in the colloidal suspension [16].

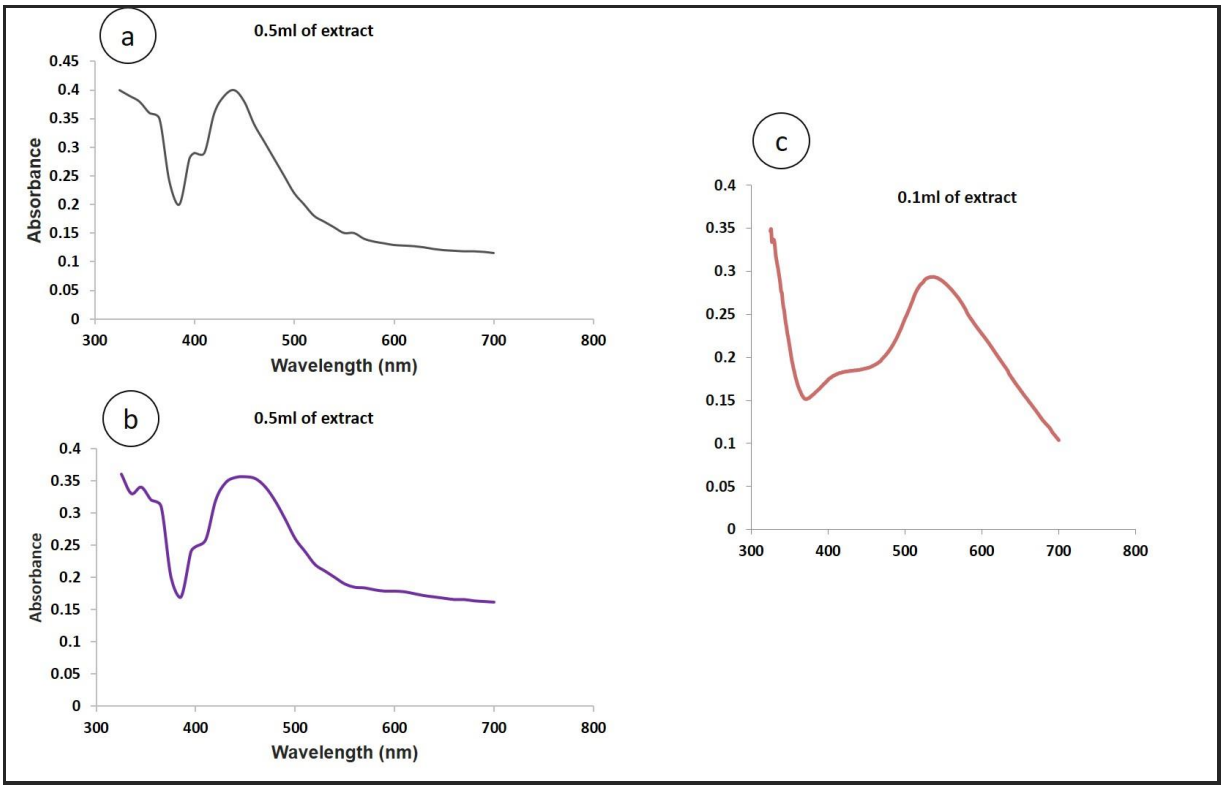

Fig. 1. UV–visible spectra of AuNPs prepared with varying volumes of *Zataria multiflora* extract: (a) 1.0 ml, (b) 0.5 ml, and (c) 0.1 ml.

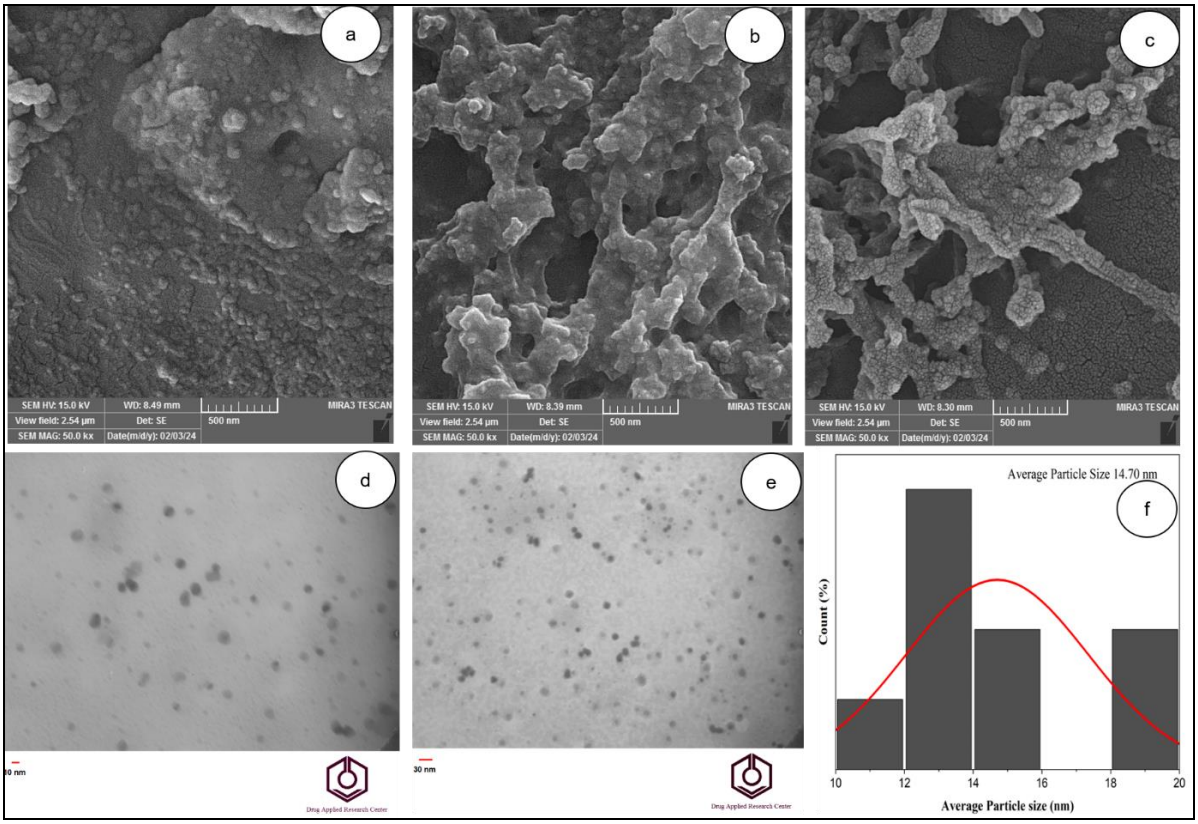

Fig. 2. (a–c) SEM images of Zataria-AuNPs; (d, e) TEM images showing uniform spherical morphology; and (f) histogram of particle size distribution based on TEM analysis.

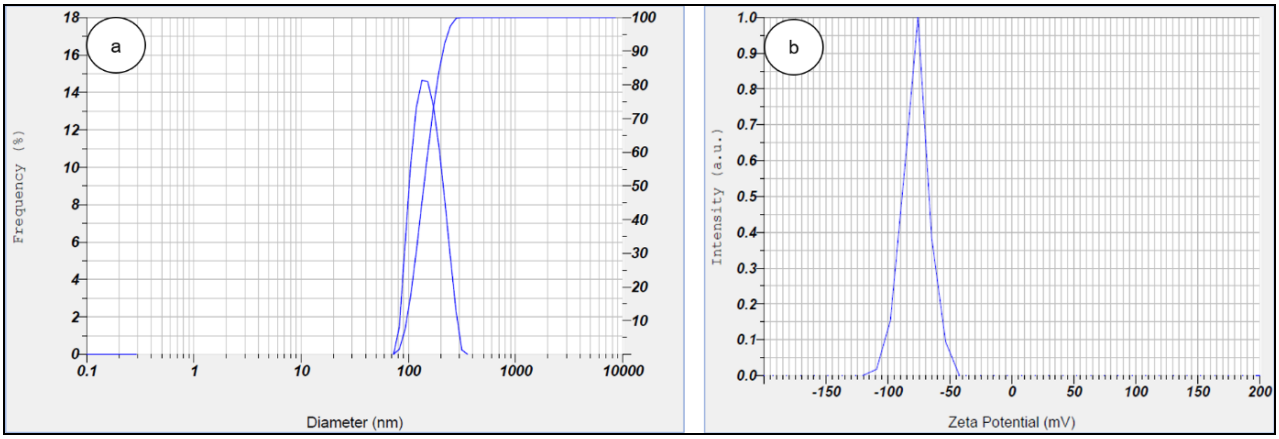

Fig. 3. (a) DLS and (b) Zeta-potential analysis of Zataria-AuNPs. The nanoparticles exhibit an average hydrodynamic diameter of 123.8 nm and a surface charge of -77.7 mV.

3.6. FTIR analysis

FTIR spectroscopy indicated the existence of functional groups on the surface of Zataria-AuNPs (Fig. 4a). Weak bands observed between 4000 – 2500 cm^{-1} indicated O–H and C–H stretching. Peaks in the 2000–1500 cm^{-1} region likely correspond to C = O and C = C bending, while those in the 1500 – 1000 cm^{-1} range suggest the presence of C–O and P–O groups. Signals in the fingerprint region (1000 – 600 cm^{-1}) may reflect C–C, C–N, and O–P. The findings suggest that hydroxyl-containing

phytochemicals are present, functioning as both reducing and stabilizing agents [14, 20].

3.7. EDAX Analysis

The presence of elemental gold was confirmed by EDAX, demonstrating the complete reduction of gold ions during nanoparticle formation. The EDAX spectrum of Au NPs exhibited a peak at 2.2 keV. Moreover, other signals, such as Cl and Ca, are seen in the analysis, which might relate to biomolecules involved in the synthesis (Fig. 4b).

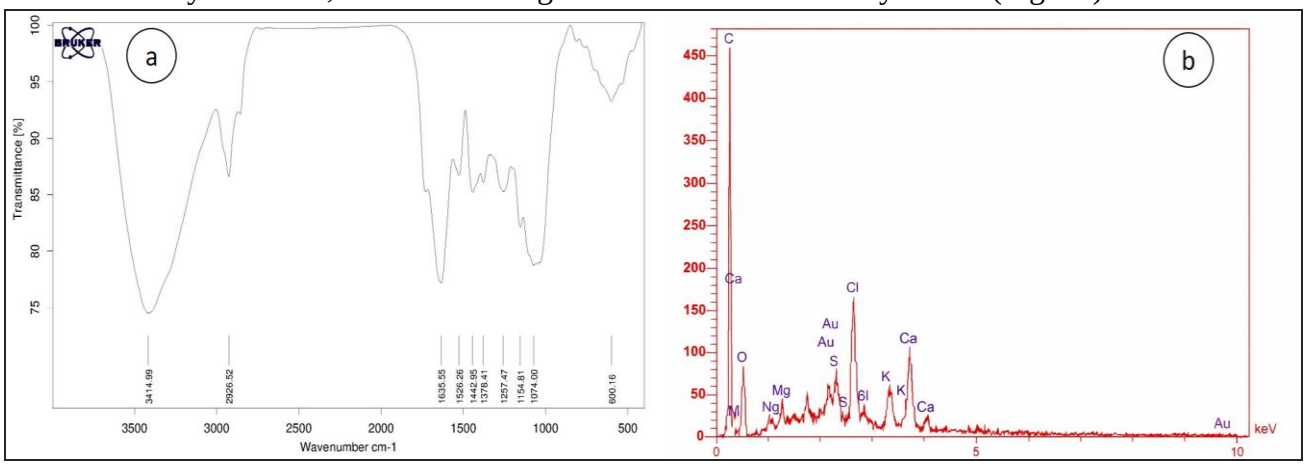

Fig. 4. (a) The FTIR spectrum of Zataria- AuNPs showing the functional groups involved in nanoparticle stabilization. (b) EDAX profile of Zataria-AuNPs. The EDAX spectrum confirm the presence of elemental gold, indicating successful reduction of gold ions.

3.8. Antibacterial activity of Zataria-AuNPs

3.8.1. Disc diffusion assay

The disk diffusion assay exhibited significant antibacterial activity of Zataria-AuNPs, which inhibited the growth of the tested bacteria, including *S. aureus* (Fig. 5a) and *E. coli* (Fig. 5b), compared to the negative control. The inhibition zones at concentrations of 100 µg/ml and above were significantly larger than the negative control ($P < 0.05$), while the positive control (antibiotic discs) exhibited the largest inhibition zones. A dose-dependent increase in inhibition zone diameter was observed for both bacteria. Detailed inhibition zone diameters for all tested concentrations are presented in Table S1 (Supplementary file).

3.8.2. MIC and MBC

The antibacterial effect of Zataria-AuNPs was assessed by determining the optical density (OD_{600}) of bacterial suspensions after 18 h of incubation with different nanoparticle concentrations (Fig. 6 a,b). A significant dose-dependent decrease in bacterial growth was observed (****P <0.0001). Based on OD and visual inspection, no bacterial growth was observed at 75 – 600 µg/ml for S. aureus and at 150 – 600 µg/ml for *E. coli.* The MIC values were determined as 75 µg/ml for S. aureus and 150 µg/ml for *E. coli*, corresponding to the lowest concentrations without visible turbidity. For MBC determination, samples from MIC wells without visible growth were transferred to fresh agar plates for subculture. No colony formation was observed at 300 and 600 µg/ml for S. aureus, whereas *E. coli* showed complete inhibition only at 600 µg/ml. Thus, the MBC values of Zataria-AuNPs were 300 µg/ml for *S. aureus* and 600 µg/ml for *E. coli*. These results indicate that S. aureus is more susceptible to Zataria-AuNPs than *E. coli.*

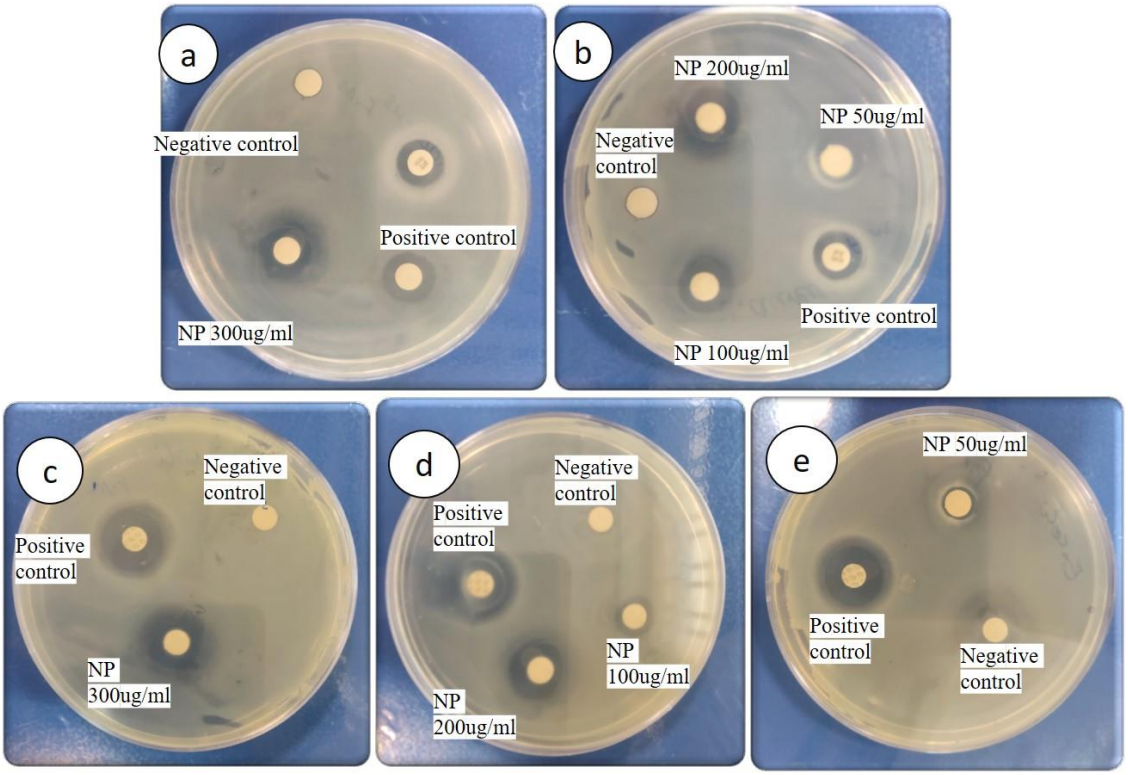

Fig. 5. Disc diffusion assay for (a, b) *S. aureus* and (c-e) *E. coli.* Discs with Zataria-AuNPs (50–300 µg/ml) were applied. A blank disc was used as the negative control; Positive controls included Tazobactam for *S. aureus* and Tobramycin for *E. coli*. (NP: Nano particle).

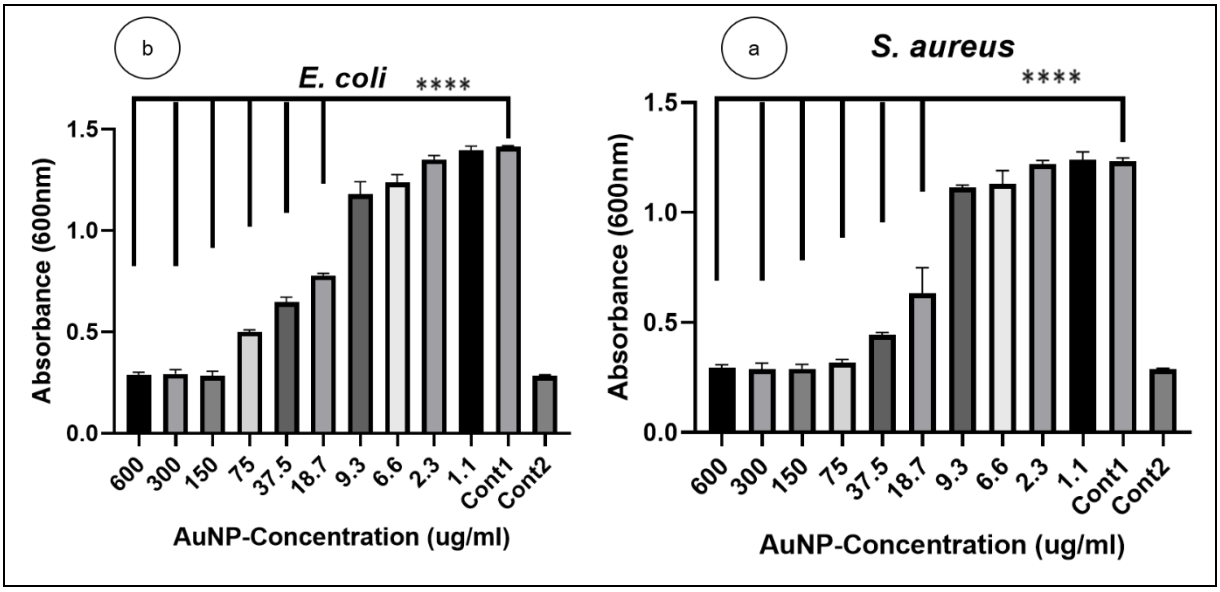

Fig. 6. Optical density (OD_{600}) of (a) *S. aureus* and (b) *E. coli* treated with different concentrations of Zataria-AuNPs after 18 h incubation. Controls: (1) untreated bacteria and (2) medium containing nanoparticles only. The MIC values were determined as the lowest concentrations showing no visible turbidity, corresponding to 75 µg/ml for *S. aureus* and 150 µg/ml for *E. coli*. Significant growth reduction was observed in treated groups (****P < 0.0001).

4. Discussion

In green synthesis of nanoparticles, plant-derived phenolics and flavonoids serve as natural reducers and stabilizers, improving nanoparticle generation and stability through antioxidant action [21, 22]. The phenolic and flavonoid contents of the aqueous extract are consistent with previous reports on *Z. multiflora*, supporting their role as reducing and stabilizing agents in synthesis of the NPs [23, 24]. Similar trends have been reported for other plants such as *Azadirachta indica* and *Ocimum sanctum*, where high phenolic and flavonoid levels facilitated efficient gold nanoparticle synthesis and improved stability [25, 26]. Although the TPC measured in this study was lower than some solvent fractions of *Z. multiflora*, it still falls within a reasonable range across Iranian *Z. multiflora* populations. The TFC of the aqueous extract in our study was comparable to values reported for hydroalcoholic extracts [27]. Studies on Iranian *Z. multiflora* populations showed TFC ranges from low to high values, while lower values have also been reported [15, 28]. Such variation may reflect differences in plant chemotypes or extraction conditions. The relatively higher TFC in our aqueous extract, compared to some earlier reports, may reflect differences in plant chemotypes or extraction conditions. Differences in extraction methods, plant origin, solvent polarity, and environmental conditions commonly explain discrepancies in TPC and TFC values.

The substantial flavonoid and phenolic contents of the extract support its antioxidant potential, given the well-established association between these compounds and free-radical scavenging activity. Results from both total antioxidant capacity and DPPH assays revealed that the extract possesses moderate antioxidant activity, supporting the presence of functional antioxidant compounds. These findings align with earlier studies on the antioxidant activity of *Z. multiflora* [24, 27].

During the synthesis reaction, a purple colouration was observed at the optimal concentration, while higher concentrations caused color shifts likely due to changes in nanoparticle size, shape, and aggregation [2]. The observed SPR peak and color indicate conditions suitable for synthesizing uniform, spherical AuNPs, consistent with previous studies using *Z. multiflora* extract [19,29]. Comparable SPR peaks have been reported for AuNPs synthesized using *Aloe vera* extract in a previous study [30], indicating that the optical properties of *Z. multiflora*–derived AuNPs fall within the typical range for plant-mediated synthesis. TEM images further confirm that the AuNPs are mainly spherical in morphology. Previous studies on *Z. multiflora* have reported similar ranges for the size of NPs [14]. SEM results showed a broader size distribution, likely due to partial aggregation during sample preparation. DLS measures the effective particle diameter in suspension, including the core, the surrounding solvation layer, and any biomolecules adsorbed from the plant extract. Consequently, differences in hydrodynamic diameter compared to microscopic methods are expected. In green synthesis studies, where surface coatings and interactions in solution affect apparent particle size, such distinctions between microscopic and dynamic light scattering techniques are commonly observed [31].

Typically, nanoparticles with Zeta-potential above +30 mV or below –30 mV experience pronounced electrostatic repulsion and good colloidal stability, which confirms good dispersion of the nanoparticles, as the strong repulsion between similarly charged particles

prevents aggregation [32]. According to reports, highly negatively charged NPs can form uniformly distributed, stable colloids in water for long periods without showing aggregation [33]. Compared to positively charged NPs, which often have a longer blood half-life, negatively charged NPs are generally less cytotoxic [16].

Hydroxyl, carbonyl, alkene, and other functional groups detected by FTIR on Zataria-AuNPs suggest the existence of phytochemicals that participate in reducing gold ions and stabilizing nanoparticles [14, 20]. Peaks often correspond to flavonoids, phenolics, and other plant-derived biomolecules [34]. The modest intensity of some signals may result from low surface concentrations or overlapping bands, limiting precise identification. Nonetheless, the FTIR profile confirms the role of bioactives in nanoparticle functionalization and capping.

Dose-dependent antibacterial effects of Zataria-AuNPs against *S. aureus* and *E. coli* were observed, indicated by the growth of inhibition zones with higher doses.

These findings are consistent with previous reports on plant-based metallic NPs, which typically show measurable inhibition in disc diffusion assays at comparable concentrations [35,36]. Gold nanoparticles synthesized using *Azadirachta indica* (Neem) have also been reported to show antibacterial or bioactive properties in previous works [25]. Zataria-AuNPs showed slightly stronger inhibition of *S. aureus* than *E. coli*, consistent with reports that gram-positive bacteria are more susceptible [13, 37]. However, studies showing greater effects on *E. coli* suggest that plant extract composition and synthesis conditions affecting nanoparticle size and surface may influence activity [19]. The nanoparticles probably disrupt the bacterial membranes by adhering to their cell walls, a mechanism seen in both gold and silver NPs [4]. The smaller inhibition zone for *E. coli* may be due to its lipopolysaccharide (LPS) layer, which provides added resistance to gram-negative bacteria. The antibacterial activity of AuNPs likely involves oxidative stress and membrane disruption. Phytochemical coatings on NPs may enhance interactions with the bacterial envelope, increasing permeability and leading to cell death [38]. Several studies on biosynthesized AuNPs have reported similar selectivity, with *S. aureus* being more susceptible than *E. coli*, which generally requires higher concentrations for inhibition [35, 37, 39]. *S. aureus* may be more susceptible because of increased nanoparticle accumulation at its peptidoglycan-rich cell wall, which can cause intracellular damage and membrane disruption. Gram-negative bacteria limit nanoparticle penetration and reduce antibacterial efficacy. Furthermore, through oxidative stress and synergistic effects, phytochemical coatings on plant-based AuNPs, such as flavonoids and phenolics, may improve antibacterial activity [38].

5. Conclusion

The successful synthesis of Zataria-AuNPs using only *Z. multiflora* aqueous extract demonstrates the key role of plant phytochemicals in reduction and stabilization. The extract concentration directly influenced nanoparticle formation. MIC results confirmed notable antibacterial activity, particularly against gram-positive strains. These findings emphasize the antimicrobial potential of Zataria-AuNPs and support their further development in biologically based antibacterial applications.

Authors' contributions

Conceptualization and Methodology: F.M, P.H, R.F; Investigation and Data analysis: F.M; Supervision: R.F, A.M; Writing the original draft: F.M; Review and editing: R.F, P.H; Administration: P.H.

Acknowledgment

This research was financially supported by Alzahra University.

Conflicts of interest

The authors have no competing interests to disclose.

References

1. Manju S and Sreenivasan K. Gold nanoparticles generated and stabilized by water soluble curcumin-polymer conjugate: Blood compatibility evaluation and targeted drug delivery onto cancer cells. *J. Colloid and Interface Sci.* 2012; 368: 144-151. doi: 10.1016/j.jcis.2011.11.024.

2. Dash S.S, Sen I.K and Dash S.K. A review on the plant extract mediated green syntheses of gold nanoparticles and its anti-microbial, anti-cancer and catalytic applications. *Int. Nano Lett*. 2021; 12(1): 47 - 66. doi: 10.1007/s40089-021-00358-6.

3. Cai F, Li Sh, Huang H, Iqbal J, Wang C and Jiang X. Green synthesis of gold nanoparticles for immune response regulation: Mechanisms, applications, and perspectives. *J. Biomed. Mater. Res.* 2021; 110(2): 1-19. doi: 10.1002/jbm.a.37281.

4. Dudhane A.A, Waghmode S.R, Dama L.B, Mhaindarkar V.P, Sonawane A and Katariya S. Synthesis and characterization of gold nanoparticles using plant extract of *Terminalia arjuna* with antibacterial activity. *Int. J. Nanosci. Nanotechnol.* 2019; 15(2): 75-82.

5. Bharadwaj K.K, Rabha B, Pati S, Sarkar T, Choudhury B.K, Barman A, Bhattacharjya D, Srivastava A, Baishya D, Edinur H.A, Abdul Kari Z and Mohd Noor N.H. Green synthesis of gold nanoparticles using plant extracts as beneficial prospect for cancer theranostics. *Molecules.* 2021; 26(21): 6389. doi: 10.3390/ molecules26216389.

6. Goshtasbi H, Awale S, Amini-Fazl M.S, Fathi M, Movafeghi A, Barar J and Omidi Y. Chitosan-graft-poly(lactide) nanocarriers: An efficient antioxidant delivery system for combating oxidative stress. *Int. J. Biol. Macromol.* 2024; 279(Pt 1): 135280. doi: 10.1016/j.ijbiomac.2024.135280.

7. Jain N, Jain P, Rajput D and Patil U.K. Green synthesized plant-based silver nanoparticles: Therapeutic prospective for anticancer and antiviral activity. *Micro Nano Syst. Lett*. 2021; 9: 5. doi: 10.1186/s40486-021-00131-6.

8. Shomali T and Mosleh N. *Zataria multiflora*, broiler health and performance: A review. *IJVR.* 2019; 20(2): 81-88. doi: 10.22099/ ijvr.2019.5250.

9. Shokri H, Asadi F, Bahonar A.R and Khosravi A.R. The role of *Zataria multiflora* essence (Iranian herb) on innate immunity of animal model. *Iran. J. Immunol.* 2006; 3: 164-168. doi: 10.22034/iji.2006.16998.

10. Huang X, Qian W, El-Sayed I.H and El-Sayed M.A. The potential use of the enhanced nonlinear properties of gold nanospheres in photothermal cancer therapy. *Lasers Surg. Med.* 2007; 39(9): 747-753. doi: 10.1002/lsm.20577.

11. Ying T-H, Yang S-F, Tsai S-J, Hsieh S-C, Huang Y-C, Bau D-T and Hsieh Y-H. Fisetin induces apoptosis in human cervical cancer HeLa cells through ERK1/2-mediated activation of caspase-8/caspase-3-dependent pathway. *Arch. Toxicol.* 2012; 86: 263-273. doi: 10.1007/s00204-011-0754-6.

12. Saed M, Ayivi R.D, Wei J and Obare S.O. Gold nanoparticles antibacterial activity: Does the surface matter? *Colloid Interface Sci. Commun.* 2024; 62: 100804. doi: 10.1016/j.colcom.2024.100804.

13. Diksha D, Gupta S.K, Gupta P, Banerjee U.C and Kalita D. Antibacterial potential of gold nanoparticles synthesized from leaf extract of *Syzygium cumini* against multidrug-resistant urinary tract pathogens. *Cureus.* 2023; 15(2): e34830. doi: 10.7759/cureus.34830.

14. Baharara J, Ramezani T, Divsalar A, Mousavi M and Seyedarabi A. Induction of apoptosis by green synthesized gold nanoparticles through activation of Caspase-3 and 9 in human cervical cancer cells. *Avicenna J. Med. Biotechnol.* 2016; 8: 75-83.

15. Meamari S, Yavari AR and Bikdeloo M. Comparison of antioxidant activity, phenolic and flavonoid contents of *Zataria multiflora* populations in Iran. *J. Med. Plants By-Prod.* 2022; 11: 101-106. doi: 10.22092/JMPB.2021. 356755.1427.

16. Gharari Z, Hanachi P and Walker T.R. Green synthesized Ag-nanoparticles using *Scutellaria multicaulis* stem extract and their selective cytotoxicity against breast cancer. *Anal. Biochem.* 2022; 653: 114786. doi: 10.1016/j.ab.2022.114786.

17. Brand-Williams W, Cuvelier M.E and Berset C. Use of a free radical method to evaluate antioxidant active. *LWT-Food Sci. Technol.* 1995; 28: 25-30. doi: 10.1016/S0023-6438(95)80008-5.

18. Hanachi P, Gharari Z, Sadeghinia H and Walker TR. Synthesis of bioactive silver nanoparticles with eco-friendly processes using *Heracleum persicum* stem extract and evaluation of their antioxidant, antibacterial, anticancer and apoptotic potential. *J. Mol. Struct.* 2022; 1265: 133325. doi: 10.1016/j.molstruc.2022.133325.

19. Muniyappan N, Pandeeswaran M and Amalraj A. Green synthesis of gold nanoparticles using *Curcuma pseudomontana* isolated curcumin: Its characterization, antimicrobial, antioxidant and anti-inflammatory activities. *Environ. Chem. Ecotoxicol.* 2021; 3: 117-124. doi: 10.1016/j.enceco.2021.01.002.

20. Saputra I.S, Saputro A.H, Apriandanu D.O.B, Permana Y.N and Yulizar Y. Novel synthesis of gold nanoparticles using *Parkia speciosa* Hassk seed extract for enhanced foam stability in hand soap. *Chem. Pap.* 2022; 76(8): 4733-4742. doi: 10.1007/s11696-022-02197-x.

21. Song J.Y, Jang H-K and Kim B.S. Biological synthesis of gold nanoparticles using *Magnolia kobus* and *Diospyros kaki* leaf extracts. *Process Biochem.* 2009; 44(10): 1133-1138. doi: 10.1016/j.procbio.2009.06.005.

22. Singh P, Kim Y-J, Zhang D and Yang D-C. Biological synthesis of nanoparticles from plants and microorganisms. *Trends Biotechnol.* 2016; 34(7): 588-599. doi: 10.1016/ j.tibtech. 2016.02.006.

23. Pourhosseini SH, Mirjalili MH, Ghasemi M, Ahadi H, Esmaeili H and Ghorbanpour M. Diversity of phytochemical components and biological activities in *Zataria multiflora* Boiss. (Lamiaceae) populations. *S. Afr. J. Bot.* 2020; 135: 148-157. doi: 10.1016/j.sajb.2020.08.024.

24. Moein S, Pimoradloo E, Moein M and Vessal M. Evaluation of antioxidant potentials and α-amylase inhibition of different fractions of Labiatae plants extracts: as a model of antidiabetic compounds properties. *Biomed. Res. Int.* 2017; 2017(1): 7319504. doi: 10.1155/2017/7319504.

25. Bindhani BK and Panigrahi AK. Green synthesis of gold nanoparticles using neem (*Azadirachta indica* L.) leaf extract and its biomedical applications. *Int. J. Adv. Biotechnol. Res.* 2014; 5: 457-464.

26. Lee SY, Krishnamurthy S, Cho C-W, Yun Y-S. Biosynthesis of gold nanoparticles using *Ocimum sanctum* extracts by solvents with different polarity. *ACS Sustain. Chem. Eng.* 2016; 4(5): 2651-2659. doi: 10.1021/ acssuschemeng.6b00161.

27. Gelehkolaei AS, Zakerimehr MR and Azizi MH. Evaluation of antioxidant and antimicrobial effects of hydroalcoholic and aqueous extracts of *Zataria multiflora* on increasing the shelf life of Lavash bread. *J. Nat. Compd. Chem.* 2022; 1(1): 33-44. doi: 10.22092/jncc.2023.129072.

28. Fatemi F, Asri Y, Rasooli I, Alipoor SD and Shaterloo M. Chemical composition and antioxidant properties of γ-irradiated Iranian *Zataria multiflora* extracts. *Pharm. Biol.* 2012; 50(2): 232-238. doi: 10.3109/ 13880209. 2011.596208.

29. Elbagory AM, Hussein AA and Meyer M. The in vitro immunomodulatory effects of gold nanoparticles synthesized from *Hypoxis hemerocallidea* aqueous extract and hypoxoside on macrophage and natural killer cells. *Int. J. Nanomedicine*. 2019; 2019(14): 9007-9018. doi: 10.2147/IJN.S216972.

30. Kamala Nalini SP, Vijayaraghavan K. Green synthesis of silver and gold nanoparticles using *Aloe vera* gel and determining its antimicrobial properties on nanoparticle impregnated cotton fabric. *J. Nanotechnol Res*. 2020; 2: 42-50. doi: 10.26502/jnr.2688-85210015.

31. Elbagory AM, Hussein AA and Meyer M. The in vitro immunomodulatory effects of gold nanoparticles synthesized from *Hypoxis hemerocallidea* aqueous extract and hypoxoside on macrophage and natural killer cells. *Int. J. Nanomedicine*. 2019; 9007-9018. doi: 10.2147/IJN.S216972.

32. Hanaor D, Michelazzi M, Leonelli C and Sorrell CC. The effects of carboxylic acids on the aqueous dispersion and electrophoretic deposition of ZrO_2. *J. Eur. Ceram. Soc.* 2012; 32(1): 235-244. doi: 10.1016/ j.jeurceramsoc. 2011.08.015

33. Balasubramani G, Ramkumar R, Krishnaveni N, Sowmiya R, Deepak P, Arul D and Perumal P. GC-MS analysis of bioactive components and synthesis of gold nanoparticle using *Chloroxylon swietenia* DC leaf extract and its larvicidal activity. *J. Photochem. Photobiol. B.* 2015; 148: 1-8. doi: 10.1016/j.jphotobiol.2015.03.016.

34. Yılmazer Keskin S, Avcı A and Fajriana Febda Kurnia H. Analyses of phytochemical compounds in the flowers and leaves of *Spiraea japonica* var. *fortunei* using UV-VIS, FTIR, and LC-MS techniques. *Heliyon*. 2024; 10(3): e25496. doi: 10.1016/j.heliyon.2024.e25496.

35. Aksoy A, Alazragi R, Alabdali AYM, Aljazzar R, El Sadi S, Alostaz M and El Hindi M. Antibacterial activity of metallic-core gold and silver nanoparticles against some animal pathogens. *Ann. Anim. Sci.* 2023; 23(2): 473-479. doi: 10.2478/aoas-2023-0008.

36. Muniyappan N, Pandeeswaran M and Amalraj A. Green synthesis of gold nanoparticles using *Curcuma pseudomontana* isolated curcumin: its characterization, antimicrobial, antioxidant and anti-inflammatory activities. *Environ. Chem. Ecotoxicol*. 2021; 3: 117-124. doi: 10.1016/j.enceco.2021.01.002.

37. Gouyau J, Duval RE, Boudier A and Lamouroux E. Investigation of nanoparticle metallic core antibacterial activity: gold and silver nanoparticles against *Escherichia coli* and *Staphylococcus aureus*. *Int. J. Mol. Sci.* 2021; 22(4): 1905. doi: 10.3390/ijms22041905.

38. Timoszyk A and Grochowalska R. Mechanism and antibacterial activity of gold nanoparticles (AuNPs) functionalized with natural compounds from plants. *Pharmaceutics*. 2022; 14(12): 2599. doi: 10.3390/ pharmaceutics14122599.

39. Sánchez-lópez E, Gomes D, Esteruelas G, Bonilla L, Lopez-machado AL, Galindo R, Cano A, Espina M, Ettcheto M, Camins A, Silva AM, Durazzo A, Santini A, Garcia ML and Souto EB. Metal-based nanoparticles as antimicrobial agents: an overview. *Nanomaterials*. 2020; 10(2): 1-43. doi: 10.3390/nano10020292.

How to cite this article: Mahmoudi F, Hanachi P, Falak R, Mohammadi A. Green synthesis and characterization of gold nanoparticles using *Zataria multiflora* extract with antibacterial activity. ***Journal of Medicinal Plants*** 2025; 24(96): 22-36.
doi: